Fabrication of hydrogenated amorphous silicon-based solar cells using RF-PECVD

Soni Prayogi, Wahyu Kunto Wibowo
Department of Electrical Engineering, Faculty of Industrial Engineering, Pertamina University, Jakarta, Indonesia

Article Info

ABSTRACT

Thin-film solar cells made of hydrogenated amorphous silicon have succeeded in crystallization technologies as a less expensive alternative because of their straightforward design, sparse material requirements, low processing temperatures, and cheap manufacturing costs. A multi-chamber plasma-accelerated chemical vapor deposition apparatus driven by radio frequency was used to create the intrinsic and extrinsic layers of the a-Si: H solar cell. Multi-chamber allows us to upgrade each layer of the gadget utilizing a distinct space, preventing cross-contamination throughout the procedure. To enhance cell conversion efficiency, a thorough analysis has been conducted in this work to evaluate the manufacturing process and comprehend the link between process factors and property dependency. Our findings demonstrate an amorphous Si: H solar cell with a maximum cell efficiency of 6.52%, Voc 880 mV, Isc 11.33 mA/cm2, and FF 65%. We think that a modeling method followed by manufacturing can further enhance the performance of a-Si: H-based solar cell devices.

Corresponding Author:

Soni Prayogi
Department of Electrical Engineering, Faculty of Industrial Engineering, Pertamina University
Jakarta, Indonesia
Email: soni.prayogi@universitaspertamina.ac.id

1. INTRODUCTION

As the necessity for renewable energy sources and utilizing the enormous power of the sun becomes more widely understood [1], It might replace fossil fuels as our primary source of energy [2], Over the past ten years, there has been an increase in interest in the creation of thin film solar cells [3]. Compared to other silicon forms [2], for instance, mixed-phase or polycrystalline Si [4], the electromagnetic spectrum's visible area has a high absorption coefficient for hydrogenated amorphous silicon (a-Si: H) [5]. As a result, it ranks as one of the most popular and cost-effective semiconductor materials for use in thin-film solar cells [6]. Accordingly, in thin-film Si solar cells [7], it is possible to make an a-Si absorber layer thinner than other types of Si [8]. However, the Staebler-Wronski effect [9], which is a-metastability [10], and Si prevent a-Si solar cells from developing efficiently [11].

In comparison to crystal silicon, the charge carriers' diffusion length in a-Si: H is significantly shorter [12]. Due to the greater defect density caused by doping, the minority carriers' diffusion length in extrinsic a-Si: H layers is substantially shorter than it is in intrinsic a-Si: H layers [13]. Due to the incredibly short diffusion length, the photo-generated carriers would all recombine before they reached the p-n junction's depletion zone in the extrinsic (doped) layers [14]. Additionally, three layers are used in the design and production of an a-Si: H solar cell p-layer for a-Si [15], an inherent i-layer [16], and an n-layer to solve the problems with p-n configuration already described [17].

An internal electric field is present across the i-layer when light hits the solar cell [18], which layer in the a-Si:H solar cell is the active layer [19]. It is inserted in the layers that are doped [20]. The electron-hole pairs generated in the intrinsic a-Si: H layer feel the internal electric field that separates electrons and holes right away [21]. The split carriers are gathered by electrodes as they move toward the extrinsic layers while being influenced by the electric field (holes toward the p-layer and electrons toward the n-layer) [22]. As a result, the efficiency of a-Si:H solar cells is significantly influenced by the band gap and i-layer conductivity [23]. Using plasma-enhanced chemical vapor deposition technology, we are doing research to produce hydrogenated amorphous silicon (a-Si:H) thin film solar cells and to gain insight into the effects of process variables on conversion efficiency.

2.   EXPERIMENTAL METHOD

Figure 1(a) shows a schematic of the layers that make up an amorphous silicon solar cell. Light can pass through the glass and indium tin oxide (ITO) in the glass superstrate configuration [24]. ITO serves as both the front contact and the window layer, allowing a high percentage of incident light to be transmitted.

The capacitive coupled multi-chamber plasma-enhanced chemical vapor deposition process (RF-PECVD), developed locally and schematically represented in Figure 1(b), was used to create the a-Si: H p-i-n solar cells. The five process chambers of the fully automated PECVD system are managed by SCADA software in conjunction with a PLC and user interface [25], are each attached to a different central transfer chamber, and they are each supported by a different magnetic arm for handling substrates. Each process chamber has a substrate heater, an adjustable electrodes-gas shower facility, and a dry mechanical pump for maintaining the required process pressure. These components are all coupled to a 300 W RF (13.56 MHz) power supply built by SEREN. A base pressure of 5×10^{-6} torr utilizing a typical turbo-roots-rotary pumping system linked to the central chamber has been created prior to each deposition.

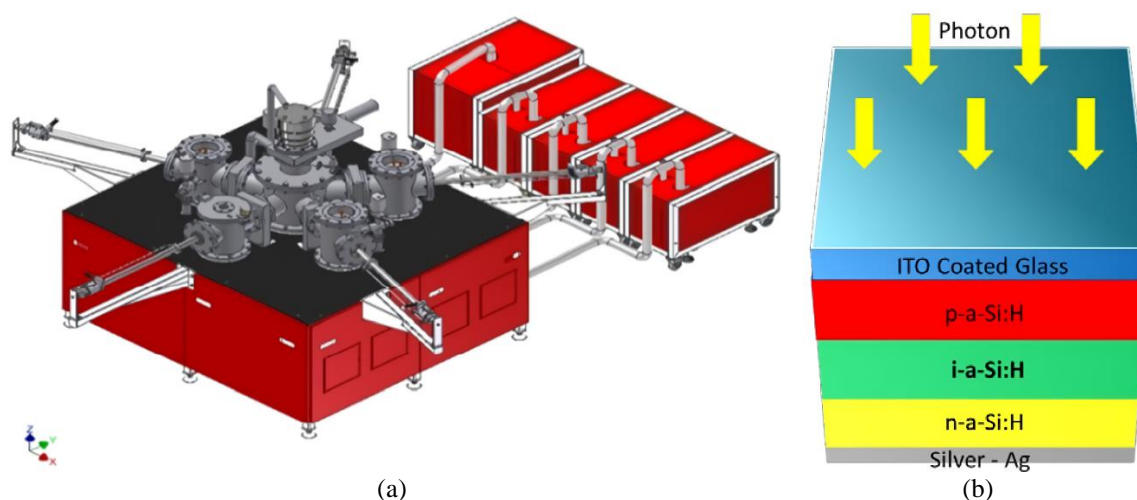(a)   (b)

Figure 1. The RF-PECVD cluster tool system: (a) diagrams the system and (b) the structure of amorphous silicon (a-Si: H) cell

This deposition system's biggest permissible substrate is 10 x 10 cm^2, and the process temperature cap is 300 °C. On a variety of glass substrates, including float glass, Schott glass, and ITO-coated glass, the development and optimization of the p-, i-, and n- layers of the a-Si: H thin film solar cell have been done in order to avoid cross-process contamination while making the device. The process variables utilized to create and enhance the individual layers as well as the a-Si: H solar cells are shown in Table 1. AFM was utilized to measure the deposited layers' thickness [26]. The electrical properties of the films were investigated by measuring co-planar conductivity using aluminum electrodes with a 12 mm length and 3 mm gap that were sputtered and evaporated. The optical spectra of the films were recorded in the 250-800 nm wavelength range using a UV-VIS spectrophotometer [27]. Coated glass substrates a-Si: H and the I-V measurements of the produced cells were evaluated using a solar simulator after layer-by-layer optimization.

Table1. Solar cells with a-Si: H p-i-n experimental parameters

Parameters	Value
Substrate and size	2.5 cm^2 of Float and ITO-coated glasses
Baseline pressure	5x10^{-6} torr
Operating temperature	250 ºC
Process gases for a-Si: H layers	p-layer: H$_2$, SiH$_4$ and B$_2$H$_6$
	i-layer: H$_2$ and SiH$_4$
	n-layer: H$_2$, SiH$_4$ and PH$_3$
Operating pressure	0.5 – 1.0 torr
Power supply	RF of 13.56 MHz at 300 W with matching network
Layer thickness	p-layer: 25 nm; i-layer: 300 nm and n-layer: 25 nm.

3. RESULTS AND DISCUSSION

The independent p-type, intrinsic, and n-type layers of the a-Si: H material were made and altered after several coating experiments to obtain the required characteristics as shown in Table 2. Utilizing foreign glass substrates with ITO coating and the best possible properties, such as an optical transmittance of 85% and a sheet resistance of 5Ω /square, and a thickness of 0.7 μ, thin film a-Si: H p-i-n solar cells have been created. Many solar cells have been created with ITO and aluminum layers as the front and back electrodes, respectively, utilizing the above-optimized individual layer deposition settings and properties as a reference in order to increase conversion efficiency with repeatability [28].

Figure 2 show I-V characteristics show that the manufactured a-Si: H thin film solar cells had a maximum cell efficiency of 6.52%, with an open circuit voltage of 880 mV, a short circuit current of 11.33 mA/cm^2, and a fill factor of 65%. To test the stability of the machine and the process, solar cells were produced continuously over the course of a single period using the best-optimized process parameters indicated in Table 2. The results are shown in Figure 2. Efficiency in this investigation varied between 6.11 and 6.52%, Voc was between 810 and 880 mV, and Jsc was between 10.89 and 11.33 mA/cm^2, and FF was between 65 and 69%, yielding an average conversion efficiency of 6.31%.

Table 2. Improved qualities of each layer of the solar cell

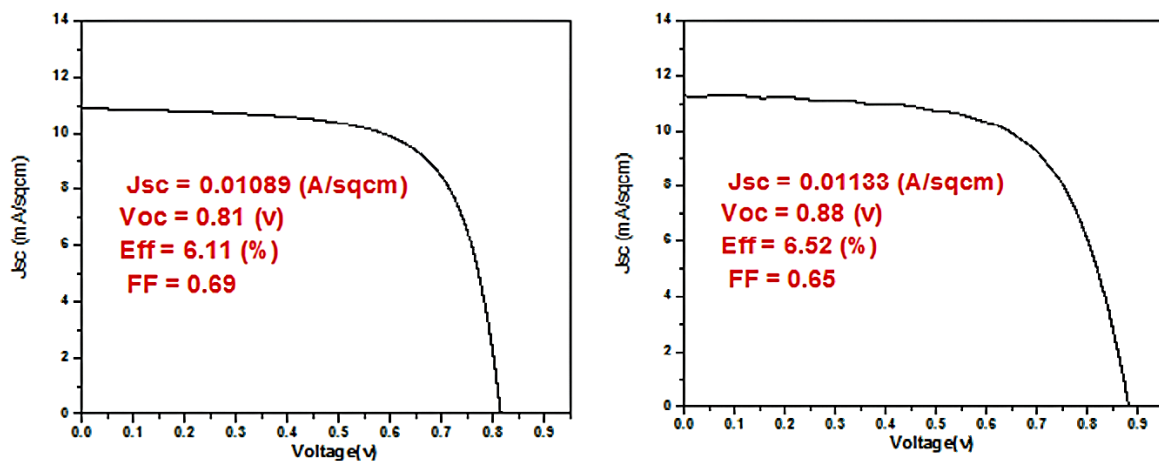| Layer	Band gap (eV)	Thickness	Conductivity
p	2.0 eV	25 nm	3.65 x 10^{-6} S cm^{-1}
i	1.6 eV	300 nm	5.63 x 10^{-5} S cm^{-1}
n	2.0 eV	25 nm	2.1x10^{-2} S cm^{-1}

Figure 2. The optimized a-Si: H solar cells' curves

Figure 3 shows the change in transmittance for thin a-Si films: H deposited with several types of coatings, including p-type, i-type, and n-type UV-VIS measurements. The film will transmit more visible light if the coating is more dilute. This indicates that as the band gap widens, the transparency of the layer will also widen [29]. Greater transparency may be caused by faults in the energy bandgap or local state decrease. There is great demand for solar cell materials with exceptional transparency, particularly intrinsic a-Si: H thin films. The optical performance of thin films may be assessed using information on visual transmission [30]. Figure 1

further demonstrates that the deposition of thinner films will result from greater variations between each layer. Fringe interference, which develops because of variations in film thickness, serves as a clue [31]. Indicating a thicker film is more interference fringes at the same wavelength interval. The interference fringe pattern observed at virtually the same layer thickness proves that the change in transmittance is not caused by the thickness of the layers [32]. Transmittance changes can be attributed to variations in crystallinity, energy gaps, Urbach energies, and particle sizes [33].
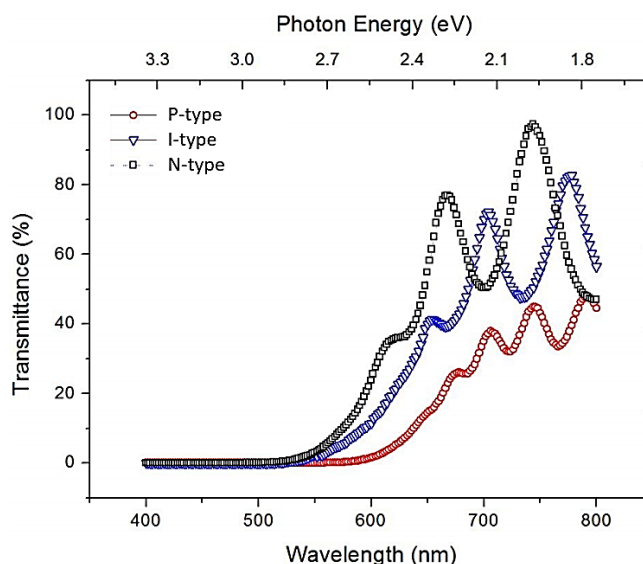

Figure 3. The transmittance of each layer is obtained

Atomic forces between the tip and the substrate will be used in AFM measurements of the sample's thickness and shape to describe the material [34]. AFMs are made up of a variety of parts, including the tip, cantilever, piezoelectric sensor, and photodetector. The tips move across the test material's surface during the material characterization procedure, changing the slope of the cantilever. The photodetector finds the slope of the cantilever. The laser beam directed to the cantilever is received by the detector, and the cantilever slope is then identified [26]. Measurements or scans are carried out at the layer and substrate boundary region (no layer). Information regarding the height difference or depth difference in this border region scan, which reveals how thick the thin layer created.

Using an AFM, each layer of p-type, i-type, and n-type semiconductors was measured, and the results are shown in Figure 4. The surface morphology of the p-type, i-type, and n-type layers are revealed in the measurement findings by the coating's surface roughness in a layer area of 2x2 μm2. We find that the p-type, i-type, and n-type strata are very uniform throughout the layers. All layers clearly showed the tiny grain size. It results from modifications in the nucleation and development of layers utilizing RF-PECVD. Value of thickness roughness of the p-type, i-type, and n-type root-mean-square (RMS) values obtained from AFM measurements were 25 nm, 300 nm, and 25 nm, respectively. Due to this incredibly high roughness value, it is feasible to increase the possibility of electron transit in each layer of the solar cell's a-Si: H [34].

Dark conductivity (σdark) and photo (σphoto) films, storage on the ITO substrate were assessed utilizing coplanar geometry and a 100 W halogen light with a power density of 100 mW/cm2. These films' photoconductivity and darkness at 300 K. Every film displays significant conductivity variations when lit [35]. For these films, the conductivity is temperature dependent. Although all films' dark and photoconductivity values were found to be almost identical at ambient temperature, i-type films had greater dark and photoconductivity values at 475 K. values for conductivity at 300 K and 475 K. In addition, the films exhibit good photosensitivity at 475 K, with the highest value for the p-type due to the enhanced structural order of these films following a single hydrogen plasma treatment step, even if the films are still amorphous in nature [36].

The intensity of the electric field produced between the p-layer and n-layer, as well as the utilization of photon energy to excite a charge carrier from the valence band to the conduction band, depend critically on the pin sample and sample p-i-n solar cell device layers, as was previously stated. More photons will be absorbed if the active layer is thicker and the rate of charge carrier generation increases [37]. But the thicker i-layer also adds to this growth due to the localized circumstances that will also increase series resistance (Rs). However, if

the i-layer is too thin, the electric field that is formed between the p-layer and the n-layer would weaken [38]. Along with series resistance, another factor that influences the characteristics of the solar cell samples is the shear resistance value (Rsh). This resistance is related to the process of charge carrier recombination from the conduction band to the valence band [39]. In the p-i-n sample solar cell, recombination between the bands is not predicted since it would decrease the electron flow (current flow) from the n-layer to the p-layer [40]. However, this issue cannot be resolved in the pin sample solar cells or the p-i-n sample due to the localized states of the a-Si: H material in the energy bandgap region, which increases the likelihood of recombination between the ribbons. Therefore, the ideal solar cell has a very high Rsh value and a very low Rs value.
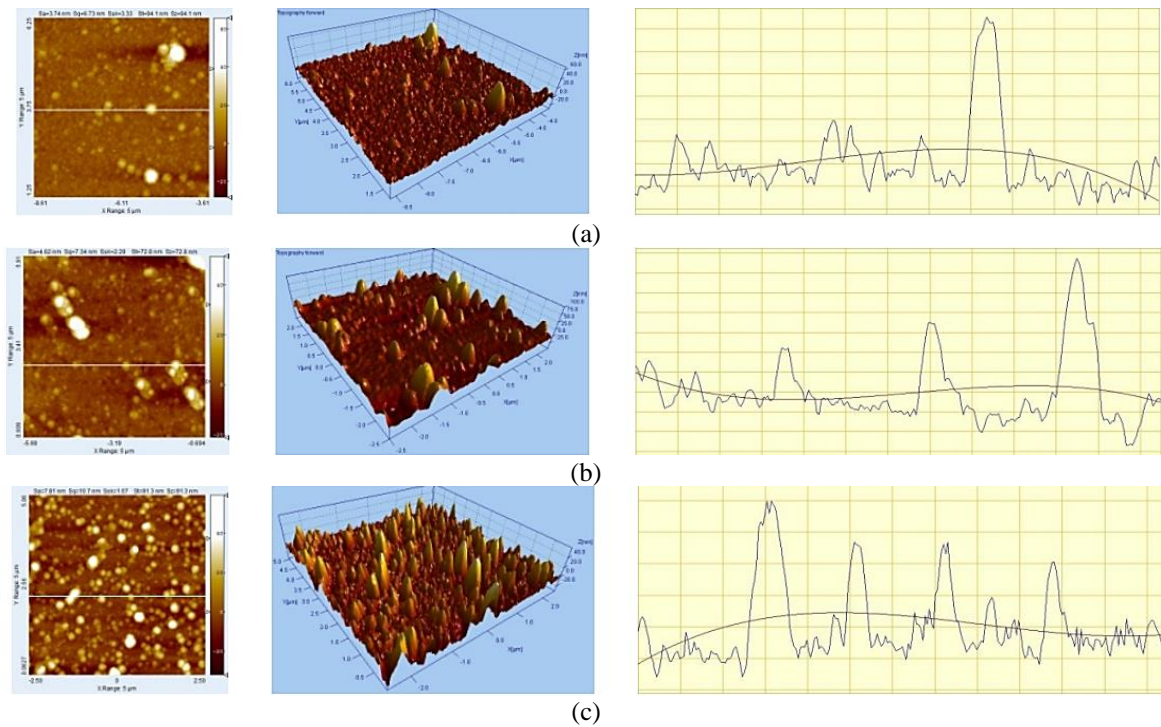

(a)

(b)

(c)

Figure 4. Morphology of the surface layer of a-Si: H using AFM: (a) p-type, (b) i-type, and (c) n-type between the ribbons

4.   CONCLUSION

In conclusion, the a-Si: H p-i-n solar cells were produced on ITO-coated glass using the multi-chamber RF-PECVD technique at a process temperature of 250 °C. The intrinsic as well as doped layers of the a-Si: H material's properties, such as electrical conductivity, optical band gap, and layer thickness, have been improved via meticulously assessing the respective doping efficiency, RF power, and deposition rate. The structure and surface appearance of the different cell layers have been examined during AFM research. The 2.5 X 2.5 cm^2 a-Si: H thin film solar cells were produced, and their I-V characteristics led to the maximum cell conversion efficiency of 6.52%, Voc of 880 mV, Jsc of 11.33 mA/cm^2, and FF of 65%. Studies on the manufacture of solar cells that focused on repeatability have shown how crucial machine design and process management are for obtaining consistent outcomes. In this instance, this was due to the multi-chamber facility, which allowed us to employ specialized chambers to optimize each of the device's distinct layers.

REFERENCES

[1]   L. Phillips, "Solar energy," in *Managing Global Warming*, Elsevier, 2019, pp. 317–332. doi: 10.1016/B978-0-12-814104-5.00009-0.
[2]   T. K. Ghosh and M. A. Prelas, "Solar Energy," in *Energy Resources and Systems*, Dordrecht: Springer Netherlands, 2011, pp. 79–156. doi: 10.1007/978-94-007-1402-1_2.

[3] F. Meng *et al.*, "Role of the buffer at the interface of intrinsic a-Si:H and p-type a-Si:H on amorphous/crystalline silicon heterojunction solar cells," *Applied Physics Letters*, vol. 107, no. 22, Nov. 2015, doi: 10.1063/1.4936196.

[4] S. C. Bhatia, "Solar devices," in *Advanced Renewable Energy Systems*, Elsevier, 2014, pp. 68–93. doi: 10.1016/B978-1-78242-269-3.50003-6.

[5] S. Prayogi, Y. Cahyono, and D. Darminto, "Electronic structure analysis of a-Si: H p-i1-i2-n solar cells using ellipsometry spectroscopy," *Optical and Quantum Electronics*, vol. 54, no. 11, p. 732, Nov. 2022, doi: 10.1007/s11082-022-04044-5.

[6] J. Krautmann and J. Zhu, "Photovoltaic Solar Energy Systems: Market Trends In The United States," *International Journal of Applied Power Engineering (IJAPE)*, vol. 1, no. 3, 2012, doi: 10.11591/ijape.v1i3.1541.

[7] S. Irvine, "Solar Cells and Photovoltaics," in *Springer Handbook of Electronic and Photonic Materials*, Boston, MA: Springer US, 2006, pp. 1095–1106. doi: 10.1007/978-0-387-29185-7_46.

[8] D. Kumar, K. P. S. Parmar, and P. Kuchhal, "Analysis of Charge Transport Properties of Dye-Sensitized Solar Cell (DSSC) with TiO2 Working Electrode by Employing Electrochemical Impedance Spectroscopy (EIS)," *International Journal of Renewable Energy Research*, vol. 11, no. 1, pp. 211–222, 2021, doi: 10.20508/ijrer.v11i1.11702.g8126.

[9] C. B. Singh, S. Bhattacharya, S. Prayogi, U. S. Patel, P. B. Bhargav, and N. Ahmed, "A new look at an explanation of band gap of PECVD grown a-Si:H thin films using absorption spectra, spectroscopic ellipsometry, Raman, and FTIR spectrosopy," *Optical Materials*, vol. 154, p. 115809, Aug. 2024, doi: 10.1016/j.optmat.2024.115809.

[10] Z. Taliashvili *et al.*, "Optical properties of periodically and aperiodically nanostructured p-n junctions," *Optical and Quantum Electronics*, vol. 55, no. 11, p. 1028, Nov. 2023, doi: 10.1007/s11082-023-05274-x.

[11] A. Illiberi, P. Kudlacek, A. H. M. Smets, M. Creatore, and M. C. M. Van De Sanden, "Effect of ion bombardment on the a-Si:H based surface passivation of c -Si surfaces," *Applied Physics Letters*, vol. 98, no. 24, 2011, doi: 10.1063/1.3601485.

[12] S. Prayogi, A. Ayunis, Y. Cahyono, and D. Darminto, "N-type H2-doped amorphous silicon layer for solar-cell application," *Materials for Renewable and Sustainable Energy*, vol. 12, no. 2, pp. 95–104, 2023, doi: 10.1007/s40243-023-00232-9.

[13] W. Duan, Y. Qiu, L. Zhang, J. Yu, J. Bian, and Z. Liu, "Influence of precursor a-Si:H dehydrogenation on the aluminum induced crystallization process," *Materials Chemistry and Physics*, vol. 146, no. 1–2, pp. 141–145, 2014, doi: 10.1016/j.matchemphys.2014.03.012.

[14] S. H. Wang, H. E. Chang, C. C. Lee, Y. K. Fuh, and T. T. Li, "Evolution of a-Si:H to nc-Si:H transition of hydrogenated silicon films deposited by trichlorosilane using principle component analysis of optical emission spectroscopy," *Materials Chemistry and Physics*, vol. 240, 2020, doi: 10.1016/j.matchemphys.2019.122186.

[15] J. Song *et al.*, "Degradation of electrical characteristics in low-bandgap polymer solar cells associated with light-induced aging," *Organic Electronics*, vol. 81, 2020, doi: 10.1016/j.orgel.2020.105686.

[16] K. Belrhiti Alaoui, S. Laalioui, Z. Naimi, B. Ikken, and A. Outzourhit, "Photovoltaic and impedance spectroscopy characterization of single-junction a-Si:H p–i–n solar cells deposited by simple shadow masking techniques using PECVD," *AIP Advances*, vol. 10, no. 9, Sep. 2020, doi: 10.1063/5.0022389.

[17] S. M. Rozati and S. A. M. Ziabari, "A review of various single layer, bilayer, and multilayer TCO materials and their applications," *Materials Chemistry and Physics*, vol. 292, 2022, doi: 10.1016/j.matchemphys.2022.126789.

[18] S. Prayogi *et al.*, "Observation of resonant exciton and correlated plasmon yielding correlated plexciton in amorphous silicon with various hydrogen content," *Scientific Reports*, vol. 12, no. 1, 2022, doi: 10.1038/s41598-022-24713-5.

[19] K. Morigaki and C. Ogihara, "Amorphous Semiconductors: Structure, Optical, and Electrical Properties," in *Springer Handbook of Electronic and Photonic Materials*, Boston, MA: Springer US, 2006, pp. 565–580. doi: 10.1007/978-0-387-29185-7_25.

[20] G. Dingemans, M. C. M. Van De Sanden, and W. M. M. Kessels, "Influence of the deposition temperature on the c-Si Surface passivation by Al2 O3 films synthesized by ALD and PECVD," *Electrochemical and Solid-State Letters*, vol. 13, no. 3, 2010, doi: 10.1149/1.3276040.

[21] K. H. Kim, E. V. Johnson, A. G. Kazanskii, M. V. Khenkin, and P. Roca, "Unravelling a simple method for the low temperature synthesis of silicon nanocrystals and monolithic nanocrystalline thin films," *Scientific Reports*, vol. 7, 2017, doi: 10.1038/srep40553.

[22] L. Ardhenta and W. Wijono, "Photovoltaic Array Modeling under Uniform Irradiation and Partial Shading Condition," *International Journal of Applied Power Engineering (IJAPE)*, vol. 6, no. 3, p. 142, 2017, doi: 10.11591/ijape.v6.i3.pp142-149.

[23] A. Bou *et al.*, "Limited information of impedance spectroscopy about electronic diffusion transport: The case of perovskite solar cells," *APL Materials*, vol. 10, no. 5, 2022, doi: 10.1063/5.0087705.

[24] P. Rakshit and N. R. Das, "Effect of device parameters on improving the quantum efficiency of a lateral Si p–i–n photodetector," *Optical and Quantum Electronics*, vol. 52, no. 8, p. 371, Aug. 2020, doi: 10.1007/s11082-020-02490-7.

[25] R. S. Zamel and A. M. A. Hussien, "Study the optoelectronic properties of reduced graphene oxide doped on the porous silicon for photodetector," *Optical and Quantum Electronics*, vol. 55, no. 11, p. 1023, Nov. 2023, doi: 10.1007/s11082-023-05399-z.

[26] R. Pedrak *et al.*, "Micromachined atomic force microscopy sensor with integrated piezoresistive sensor and thermal bimorph actuator for high-speed tapping-mode atomic force microscopy phase-imaging in higher eigenmodes," *Journal of Vacuum Science & Technology B: Microelectronics and Nanometer Structures Processing, Measurement, and Phenomena*, vol. 21, no. 6, pp. 3102–3107, 2003, doi: 10.1116/1.1614252.

[27] A. J. Flewitt, "Hydrogenated Amorphous Silicon Thin-Film Transistors (a-Si:H TFTs)," in *Handbook of Visual Display Technology*, Cham: Springer International Publishing, 2016, pp. 887–909. doi: 10.1007/978-3-319-14346-0_47.

[28] L. Changshi, "The Most Reliable and Precise Model to Determine Schottky Barrier Height and Photoelectron Yield Spectroscopy," *Optical and Quantum Electronics*, vol. 51, no. 11, p. 370, Nov. 2019, doi: 10.1007/s11082-019-2088-1.

[29] M. Venkateshkumar and R. Raghavan, "Hybrid Photovoltaic and Wind Power System with Battery Management System Using Fuzzy Logic Controller," *International Journal of Applied Power Engineering (IJAPE)*, vol. 5, no. 2, p. 72, Aug. 2016, doi: 10.11591/ijape.v5.i2.pp72-78.

[30] Q. Wang *et al.*, "p-type c-Si/SnO2/Mg heterojunction solar cells with an induced inversion layer," *Applied Physics Letters*, vol. 119, no. 26, Dec. 2021, doi: 10.1063/5.0070585.

[31] R. C. Chittick, J. H. Alexander, and H. F. Sterling, "The Preparation and Properties of Amorphous Silicon," *Journal of The Electrochemical Society*, vol. 116, no. 1, p. 77, 1969, doi: 10.1149/1.2411779.

[32] R. E. Welser, S. J. Polly, M. Kacharia, A. Fedorenko, A. K. Sood, and S. M. Hubbard, "Design and Demonstration of High-Efficiency Quantum Well Solar Cells Employing Thin Strained Superlattices," *Scientific Reports*, vol. 9, no. 1, 2019, doi: 10.1038/s41598-019-50321-x.

[33] S. Baskar and R. Pratibha Nalini, "Synthesis and characterization of silicon nanocrystals in SiC matrix using sputtering and PECVD techniques," *Materials Today: Proceedings*, vol. 3, no. 6, pp. 2121–2131, 2016, doi: 10.1016/j.matpr.2016.04.117.

[34] A. Dzedzickis *et al.*, "Modification of the AFM sensor by a precisely regulated air stream to increase imaging speed and accuracy in the contact mode," *Sensors (Switzerland)*, vol. 18, no. 8, 2018, doi: 10.3390/s18082694.

[35] C. Burgess, "Optical Spectroscopy | Detection Devices*," in *Encyclopedia of Analytical Science*, Elsevier, 2005, pp. 438–443. doi: 10.1016/B0-12-369397-7/00431-3.

[36] A. Pan and X. Zhu, "Optoelectronic properties of semiconductor nanowires," in *Semiconductor Nanowires*, Elsevier, 2015, pp. 327–363. doi: 10.1016/B978-1-78242-253-2.00012-8.

[37] J. P. Colinge and C. A. Colinge, "Energy Band Theory," in *Physics of Semiconductor Devices*, Boston: Kluwer Academic Publishers, 2005, pp. 1–49. doi: 10.1007/0-306-47622-3_1.

[38] J. P. Colinge and C. A. Colinge, "Theory of Electrical Conduction," in *Physics of Semiconductor Devices*, Boston: Kluwer Academic Publishers, 2012, pp. 51–72. doi: 10.1007/0-306-47622-3_2.

[39] A. G. Djafar and Y. Mohamad, "Method to assess the potential of photovoltaic panel based on roof design," *International Journal of Applied Power Engineering (IJAPE)*, vol. 11, no. 3, p. 186, Sep. 2022, doi: 10.11591/ijape.v11.i3.pp186-198.

[40] S. Prayogi, Y. Cahyono, I. Iqballudin, M. Stchakovsky, and D. Darminto, "The effect of adding an active layer to the structure of a-Si: H solar cells on the efficiency using RF-PECVD," *Journal of Materials Science: Materials in Electronics*, vol. 32, no. 6, pp. 7609–7618, 2021, doi: 10.1007/s10854-021-05477-6.

BIOGRAPHIES OF AUTHORS

Dr. Soni Prayogi, M.Si. is currently works as Electrical Engineering, Pertamina University, Indonesia. He does research in materials science, condensed matter physics, magnetic compounds, and nano-/2D-materials. His group's current project is 'Development of carbon-based materials from 'green' sources of carbon and functional materials from natural resources' for electronic and magnetic applications. He can be contacted at email: soni.prayogi@universitaspertamina.ac.id.

Dr. Eng. Wahyu Kunto Wibowo is received a Bachelor of Engineering degree from the Electrical Engineering Study Program at Diponegoro University, Semarang. Then he received a Master of Engineering and Doctor of Engineering degree from the Interdisciplinary Program of Mechatronics Engineering at Pukyong National University, Busan, South Korea. As work experience, he has been involved in several projects including PLN Semarang customer satisfaction surveyor, automotive safety for power windows, and electric propulsion system for small ships. He started joining Pertamina University in 2016 and is currently focusing on the areas of electrical machine control, energy conversion, and high voltage engineering. He can be contacted at email: wahyu.kw@universitaspertamina.ac.id.